Cancer Immunol Immunother (2005) 54: 1200–1213
DOI 10.1007/s00262-005-0693-2

ORIGINAL ARTICLE

**Angela Coliva · Alberto Zacchetti · Elena Luison
Antonella Tomassetti · Italia Bongarzone
Ettore Seregni · Emilio Bombardieri · Franck Martin
Augusto Giussani · Mariangela Figini · Silvana Canevari**

^{90}Y Labeling of monoclonal antibody MOv18 and preclinical validation for radioimmunotherapy of human ovarian carcinomas

Received: 2 December 2004 / Accepted: 18 February 2005 / Published online: 31 May 2005

Abstract The monoclonal antibody (mAb) MOv18 binds the membrane alpha isoform of the folate receptor (FR) which is overexpressed in human ovarian carcinoma cells. Exploiting the targeting capacity of this mAb, we developed and preclinically validated a protocol for the stable labeling of the mAb with ^{90}Y, an isotope which has shown promise in cancer radioimmunotherapy. MOv18 was derivatized with the stable macrocyclic ligand *p*-isothiocyanatobenzyl-1,4,7,10-tetraazacyclododecane-1,4,7,10- tetraacetic acid (Bz-DOTA). MOv18-Bz-DOTA conjugates were labeled with ^{90}Y or ^{111}In under metal-free and good laboratory practice conditions. At the optimal Bz-DOTA/mAb derivatization ratio of 4–5, conjugates maintained binding activity up to 6 months, were efficiently labeled with ^{90}Y or ^{111}In (mean labeling yield 85 and 64%, associated to a final mean specific activity of 74 and 37 MBq/mg) and displayed a mean immunoreactivity of 60 and 58%, respectively. The radiolabeled preparations were stable in human serum, with >97% radioactivity associated to mAb at 48 h after labeling. The ability of ^{90}Y- and ^{111}In-MOv18 to localize FR on tumors in vivo was analyzed in nude mice bearing tumors induced by isogenic cell lines differing only in the presence or absence of the relevant antigen [A431FR (FR-positive) and A431tMock (FR-negative)]. In vivo biodistribution in organs other than tumor was comparable in non-tumor-, A431tMock- and A431FR-bearing mice, whereas the median tumor uptake of the radiolabeled reagents, expressed as area under the curve (AUC) and maximum uptake (U_{max}), was significantly higher (sixfold to sevenfold) in A431FR than in A431tMock tumors ($P = 0.0465$ and $P = 0.0332$, respectively). Mean maximum uptake (% ID/g) for ^{90}Y-MOv18 was 53.7 and 7.4 in A431FR and A431tMock respectively; corresponding values for ^{111}In-Mov18 were 45.0 and 11.3. These data demonstrate the feasibility of ^{90}Y-labeling of MOv18 without compromising antibody binding ability and the immunoreagent-specific localization in vivo on FR-expressing tumors, suggesting the suitability of ^{90}Y-MOv18 for clinical studies.

Keywords Monoclonal antibody MOv18 · Chelates · ^{90}Y · Preclinical model · Ovarian cancer radioimmunotherapy

Abbreviations mAb: Monoclonal antibody · FR: Alpha isoform of the folate receptor · Bz-DOTA: *p*-isothiocyanatobenzyl-1,4,7,10-tetraazacyclododecane-1,4,7,10-tetraacetic acid · GLP: Good laboratory practice · % ID/g: Percent injected dose/g · AUC: Area under the curve · U_{max}: Maximum uptake · HSA: Human serum albumin · SDS-PAGE: Sodium dodecyl sulfate polyacrylamide gel electrophoresis · MALDI-TOF-MS: Matrix-assisted laser desorption/ionization

Angela Coliva and Alberto Zacchetti contributed equally to this work.

A. Coliva · E. Seregni · E. Bombardieri
Unit of Nuclear Medicine, Istituto Nazionale Tumori, via Venezian 1, 20133 Milano, Italy

A. Zacchetti · E. Luison · A. Tomassetti · M. Figini
S. Canevari (✉)
Unit of Molecular Therapies, Department of Experimental Oncology, Istituto Nazionale Tumori, via Venezian 1, 20133 Milano, Italy
E-mail: silvana.canevari@istitutotumori.mi.it
Tel.: +39-02-23902567
Fax: +39-02-23903073

I. Bongarzone
Molecular Mechanisms of Cancer Growth and Progression, Istituto Nazionale Tumori, via Venezian 1, 20133 Milano, Italy

F. Martin
Dompe' S.p.a., L'Aquila, Italy

A. Giussani
Physics Department, Università degli Studi di Milano, Milano, Italy

time-of-flight mass spectrometry · L/P: Ligand/protein ratio · FITC: Fluorescein-isothiocyanate · DTPA: Diethylenetriaminepentaacetic acid · EDTA: Ethylenediaminetetraacetic acid · ITLC: Instant thin layer chromatography

Introduction

Ovarian cancer remains a major health problem in the United States and most Western European countries. The standard therapeutic approach for ovarian carcinoma consists of radical surgery followed by different chemotherapy regimens. Despite the availability of several effective chemotherapeutic agents for the treatment of ovarian cancer, survival is still poor. Front-line chemotherapy leads to complete responses in about 50–70% of patients, but the rate of relapse is very high and second-line chemotherapy is not always successful [22, 32]. This problem points to the need for anticancer drugs with mechanisms of cancer toxicity different from those of the currently available chemotherapy agents. Thus, new treatment modalities have been developed, most of which are based on the targeting ability of monoclonal antibodies (mAb) that detect tumor-associated antigens.

The alpha isoform of the folate receptor (FR) is one of the more promising targets for ovarian carcinoma. This receptor, identified by mAbs MOv18 and MOv19 produced in our laboratory [28], is a 38–40 kDa glycosylphosphatidylinositol-anchored molecule [9] in the family of homologous proteins that bind folic acid with high affinity. The receptor is homogeneously overexpressed in the majority of ovarian carcinomas and is associated with signaling molecules in specific membrane subregions [30]. Moreover, FR expression correlates with progression of the disease [37]. FR gene transfection confers a proliferative advantage to cells [4] and functional downregulation of the membrane expression of FR in ovarian cancer cells is accompanied by a partial reversion of the transformed phenotype [17].

The mAb MOv18 has been characterized in several preclinical studies in vitro and in vivo [4, 9, 17, 19, 30, 28, 37]. In more than 100 patients evaluated by scintigraphy for diagnostic purposes, using mAb MOv18 labeled with ^{131}I or a two-step procedure, lesions expressing the target antigen were detected with high specificity (97%) and good sensitivity (85%) [5, 10, 33]. A pilot study to evaluate the therapeutic potential of ^{131}I-MOv18 also gave encouraging results, since a single intraperitoneal administration of a total activity of 3.7 GBq (100 mCi) through this reagent [11] resulted in complete long term remission in five of 16 treated patients. More recent studies with the chimeric variant of MOv18 labeled with ^{131}I further support the therapeutic potential of the antibody [39, 40].

In recent years, radioimmunotherapy has gained a role in cancer treatment because of its success in lymphoma patients and the recent approval of ^{90}Y or ^{131}I radiolabeled-anti CD20 mAb by the United States Food and Drug Administration [3, 8]. However, a broader application of this technology to carcinomas awaits proof of safety and efficacy in a clinical setting. The selection of a radionuclide that delivers sufficient radiation energy to kill carcinomas, which present limited radiosensitivity compared with hematologic malignancies, is a major concern. Selection considerations include the type of isotope and its associated emission characteristics as well as the clinical context. Although several radioisotopes have been considered for radioimmunotherapy and the relative merits of beta or alpha emitters have been extensively discussed [8, 20, 35], most attention has focused on the use of ^{131}I ($T_{1/2}$ = 8.05 days, E_{γ} = 0.364 MeV, $E_{\beta max}$ = 0.61 MeV, max tissue penetration = 2.4 mm) and ^{90}Y ($T_{1/2}$ = 2.67 days, $E_{\beta max}$ = 2.27 MeV, max tissue penetration = 11.9 mm). The energy and maximal tissue penetration of the beta particles emitted by ^{90}Y are considerably higher as compared with ^{131}I so that ^{90}Y can deposits a greater radiation dose over a much larger distance [8]. Moreover, since ^{90}Y has no gamma component, both shielding of hospital personnel and use of high patient doses without prolonged or any hospital stay after administration are easily managed.

In light of the favourable physical characteristics of ^{90}Y with respect to potential cytotoxicity to evident tumor masses, and because ovarian carcinoma is a disease, mainly confined to the peritoneal cavity, but frequently present as multiple solid deposits of variable dimensions we focused on the development of a ^{90}Y-MOv18 conjugate as a radioimmunotherapeutic reagent for eventual clinical use. Furthermore, evidence of anti-tumor activity of other intraperitoneally administered ^{90}Y-radiolabeled mAbs in ovarian cancer patients has been reported [1, 16]. Here we describe the optimization of procedures to obtain functional ^{90}Y-MOv18 suitable for clinical application. Using an appropriate mathematical procedure and a suitable preclinical model, we demonstrate the strong and specific localization of this radiolabeled reagent.

Materials and methods

Chemicals and reagents

Bz-DOTA was purchased from Macrocyclics (Dallas, TX, USA). Human serum albumin (HSA) (25% w/v, USP) was obtained from Kedrion (Castelvecchio Pascoli, Italy). Ascorbic acid as a sterile and apyrogenic solution (200 mg/ml) was purchased from Bracco (Milan, Italy). All other chemicals were high-purity grade (Sigma). ^{90}Y and ^{111}In were purchased from Perkin Elmer Life and Analytical Sciences, Inc. (Boston, MA, USA). All glassware was washed with 2 M HCl and MilliQ water (Waters, Milford, MA, USA) (resistivity at 25°C 10–18 MeOhm/cm) to avoid metal contamination. Buffers were aseptically filtered through 0.22-μm mem-

branes and stored at room temperature in sterile conditions. Disposable PD-10 desalting columns (Amersham Pharmacia Biotech, Uppsala, Sweden) were washed with 0.5 M NaOH for sanitization and with 0.5 M HCl to remove heavy metal cations.

Antibody

The mAb MOv18 (IgG1k) was generated against a human ovarian cancer specimen [28]. A master cell bank was prepared by Sorebio (Martillac, France), starting from a batch of hybridoma cells certified for identity, sterility and viral absence by RBM SpA (Colleretto Giacosa, Italy). Sorebio prepared and certified a batch of purified MOv18 antibody in clinical grade condition at a concentration of 10 mg/ml. Preliminary testing (see below) indicated that the optimal concentration was higher (>50 mg/ml). Thus, for use in a future clinical trial, the 10 mg/ml antibody batch was adequately concentrated by Areta International S.r.l (Gerenzano, Italy), a facility qualified in the production and certification of biological products for clinical use. The final mAb preparation (51 mg/ml, 0.34 mM) retained all binding activity and specificity, as assayed by immunofluorescence, ELISA and Western blotting, and presented $<1\%$ of aggregates as determined by analytical HPLC gel filtration. Unmodified antibody concentration was assessed by UV absorbance at 280 nm, while Bz-DOTA-mAb concentration was determined by BCA protein assay (Pierce Biotechnology, Rockford, IL, USA).

Cell lines

The following mycoplasma-free human tumor cell lines were used: ovarian carcinoma IGROV1 (gift from Dr. J. Bénard, Institute Gustave Roussy, Villejuif, France); epidermoid carcinoma A431 [provided by the American Type Culture Collection (ATCC, Manassas, VA)]; and melanoma MeWo [18]. A431 cells were used to generate two isogenic lines differing only in the presence or absence of the relevant target antigen (FR) recognized by mAb MOv18. Briefly, A431 cells (3×10^4) were seeded in a 96-well plate and transfected with plasmid pRC/P10 containing the full-length FR cDNA [15] by Lipofectin (Gibco BRL, Gattesburg, MA, USA) essentially as suggested by the manufacturer. In parallel, A431tMock cells were obtained by transfection with the empty vector pRC/CMV (Invitrogen, San Diego, CA, USA). Stable transfectants were selected using 800 μg/ml of G418 (Gibco BRL), and a high FR-expressing clone (A431FR) was identified by immunofluorescence analysis using MOv18. The stable insertion of FR or of the empty vector did not modify transfectant in vitro or in vivo growth rates, which were superimposable on those of the parental A431 cells.

Tumor cell lines were maintained in RPMI-1640 (Sigma, St. Louis, MO, USA) supplemented with 10% (v/v) fetal calf serum (Sigma) and 2 mM L-glutamine (Sigma) and, in the case of transfected cells, with 800 μg/ml of G418. All cell lines were routinely tested for mycoplasma contamination using a mycoplasma polymerase chain reaction-enzyme-linked immunoassay kit (Roche, Basel, Switzerland).

Preparation of Bz-DOTA conjugates

Conjugates were derived essentially as described by Kukis et al. [23] with appropriate modifications in molar excess of Bz-DOTA to mAb used (5–25), mAb concentration (10–75 mg/ml) and reaction buffer choice (sodium carbonate or tetramethylammonium phosphate). In the optimized conditions, antibody (51 mg/ml, 0.34 mM) was incubated with a 6- to 12-fold molar excess of Bz-DOTA in 0.1 M sodium carbonate pH 9, adjusting pH with Me_4NOH (final concentration 80–90 mM) for 45 min at 37°C. Bz-DOTA conjugates were purified by gel filtration chromatography on disposable PD-10 desalting columns and eluted with 0.5 M $AcONH_4$ at pH 7.5 or 5.5 depending on the subsequent radiolabeling with ^{90}Y or ^{111}In. The final solution was filtered through 0.22-μm membranes (Waters) and stored under sterile conditions at 2–8°C. Conjugates were examined by sodium dodecyl sulfate-polyacrylamide gel electrophoresis (SDS-PAGE) in homogeneous 7.5% polyacrylamide gels using a Phast System (Amersham Pharmacia Biotech) to verify conjugate integrity.

Determination of Bz-DOTA/mAb ratio

Bz-DOTA conjugates were characterized using matrix-assisted laser desorption/ionization time-of-flight mass spectrometry (MALDI-TOF-MS) (Voyager-DE Biospectrometry Workstation, PerSeptive Biosystems, Framingham, MA, USA) with unmodified mAb MOv18 as a reference. The MALDI-TOF-MS apparatus was equipped with a pulsed nitrogen laser (330 nm) in the positive ion detection mode. Samples of mAb and Bz-DOTA-mAb were each mixed with a UV absorbing matrix prepared by dissolving 3,5-dimethoxy-4-hydroxycinnamic acid (sinapinic acid) (10 mg/ml) in a solvent of 50% acetonitrile in water containing 0.2% of trifluoroacetic acid. Mass spectra of unmodified mAb and Bz-DOTA-mAb were obtained at threshold laser irradiance for 100 shots in the linear mode at 25 kV. The mono-protonated $(M+H)^+$ form of the molecules (M) was used to determine the ligand/protein ratio (L/P) of each conjugate as:

$$L/P = \frac{(\text{Bz - DOTA - mAb conjugate molecular weight}) - (\text{mAb molecular weight})}{\text{Bz - Dota molecular weight}}$$

Evaluation of Bz-DOTA-mAb binding

Titrated doses of unmodified or conjugated antibody (from 10 μg/ml to 0.1 μg/ml) were added to 5×10^5 cells expressing FR (IGROV1 or A431FR) or non-expressing (MeWo or A431tMock) in 100 μl of PBS-0.03% bovine serum albumin, and incubated for 30 min at 0°C. Antibody binding was detected by a fluorescein-isothiocyanate (FITC)-conjugated secondary antibody (KPL) for 30 min at 0°C. For each sample, 5,000 cells were analyzed with a FACS Excalibur using Lysys II Software (Becton Dickinson) and mean fluorescence intensity (MFI) recorded. The functionality of the Bz-DOTA-mAb conjugates is given as % MFI relative to that of the unmodified mAb.

Radiolabeling

In optimized ^{90}Y radiolabeling, the desired radioactivity of yttrium in 0.05 M HCl was added to the Bz-DOTA conjugate in 0.5 M $AcONH_4$ at pH 7.5, at a concentration of 7–10 mg/ml (50–70 μM) to achieve a specific activity in the range of 37–111 MBq/mg. The labeling mixture was incubated at 37°C for 30 min in the presence of ascorbic acid at a final concentration of 10 mg/ml, brought to 1 mM final concentration of DTPA by addition of a 20 mM diethylenetriaminepentaacetic acid (DTPA) solution at pH 7.5, and incubated for 15 min at 37°C. ^{111}In radiolabeling was carried out similarly, except that the specific activity was 18–74 MBq/mg, ethylenediaminetetraacetic acid (EDTA) was used instead of DTPA, the reaction time was 60 min and the pH was 5.5. ^{90}Y-Bz-DOTA-mAb was purified by gel filtration chromatography on disposable PD-10 desalting columns equilibrated and eluted with 100 mM sodium phosphate, pH 7.4, 150 mM NaCl, 10 mg/ml ascorbic acid and 2% HSA. Ascorbic acid as a radioprotectant during ^{111}In labeling was not added because the ^{111}In-emitted energy was not radiolytic. Products were filtered through a sterile 0.22-μm membrane and activities were measured with the dose calibrator ISOMED 2000 (Elimpex, Moedling, Austria) and a COBRA II Auto-Gamma counter (Packard, PerkinElmer, Boston, MA, USA). Radiolabeled mAbs were examined by SDS-PAGE in homogeneous 7.5% polyacrylamide gels in non-reducing conditions using the Phast System (Amersham Pharmacia Biotech) and radiolabeled materials were visualized by autoradiography.

Radioisotope incorporation into the Bz-DOTA-mAb complex was assessed, before final gel filtration, by instant thin-layer chromatography (ITLC) on silica gel-impregnated glass fiber sheets (Pall Life Sciences) using a solution containing equal volumes of 10% (w/v) aqueous ammonium acetate and methanol as the mobile phase. In these conditions, protein-Bz-DOTA conjugates remain at the origin, whereas the radioisotopes chelated by EDTA or DTPA migrate to Rf 0.4–0.8. ITLC plates were exposed with a Cyclone Storage Phosphor System and analyzed by Optiquant Image Analysis Software (Packard).

Immunoreactivity of radiolabeled MOv18

Cells (duplicate samples in dilutions from 2×10^6 to 3.1×10^4) were incubated for 3 h at 0°C with trace amounts of radiolabeled mAb in 50 μl of 0.03% bovine serum albumin in PBS. Non-specific binding was evaluated in the presence of a large excess of unlabeled Bz-DOTA-mAb (final concentration 500 μg/ml). Cells were washed three times with cold medium and assessed for radioactivity in a gamma counter using an appropriate window set for ^{90}Y and ^{111}In (0–500 and 80–280 keV, respectively). The immunoreactive fraction of antibodies was calculated according to the method of Lindmo et al. [25].

In vitro stability

Purified ^{90}Y-Bz-DOTA-mAb or ^{111}In-BZ-DOTA-mAb at 1.5–2.5 μM were diluted in 500 μl fresh human serum and incubated at 37°C for 48 h. SDS-PAGE was used to control for any potential transchelation reaction with serum proteins. The percent radioactivity associated with the antibody was determined by ITLC analyses after addition of DTPA or EDTA (1 mM final concentration).

Apyrogenicity and sterility

Bz-DOTA-conjugates and the radiolabeled mAb conjugates were filtered on a 0.22-μm membrane. To demonstrate the sterility of the filtration unit, the filter upon usage was rinsed with a sterile 1% peptone solution, pH 7.1, and the peptone filtrate was incubated at 37°C for 48 h. Pyrogen contamination was evaluated by a Quantitative Chromogen LAL test (Bio Whittaker), which utilizes a modified Limulus Amebocyte Lysate and a synthetic color-producing substrate to detect endotoxin chromogenically. Endotoxin concentration was calculated from a standard curve constructed using an endotoxin standard solution.

In vivo experiments

All protocols were approved by the Ethics Committee for Animal Experimentation of the National Cancer Institute of Milan and carried out according to institutional guidelines [38]. Female CD1 *nu*/*nu* mice (athymic) were obtained at 5–6 weeks of age from Charles River Laboratories (Calco, Italy). After 1 week of acclimatization, mice were xenografted subcutaneously with 3.5×10^6 A431FR or A431tMock cells in 0.1 ml of 0.9%

NaCl. Two to three weeks after tumor cell injection, mice were randomly divided into groups and injected intravenously in the lateral tail vein with the radiolabeled antibody. Table 1 outlines design for each experiment (number of animals per group, total dose with specific activity injected, and interval times at which tissue/organs were measured).

Imaging

Six tumor-bearing mice (three with A431FR and three with A431tMock) from the $1-^{111}$In experiment were anesthetized using a combination of pentobarbital and medetomidine (35 and 10 mg/kg intraperitoneally, respectively). Time-dependent localization of the radiolabeled mAb was determined by scintigraphy (Picker Prism 1000 gamma camera, with a MEGP collimator - 6/8 inch crystal) at 3, 24, 48, 120 h after injection and static images were acquired in 15 min.

Biodistribution and localization

Four experiments were carried out with ^{90}Y- and a single experiment with ^{111}In-labeled mAb; in the $4-^{90}$Y experiment, non-tumor bearing mice were also analyzed. Biodistribution studies were carried out at multiple time points following injection (see Table 1). After dissection, tumors and other tissue/organs (spleen, kidney, liver, sternum, lungs, heart and muscle) were collected and wet-weighted. Radioactivity associated with each tissue was assessed with a gamma counter with internal standards (5 and 10 µl of the injected solution). Measurements were expressed as percentage of the injected dose per unit mass of organ (% ID/g) and as tissue/organ:-blood ratio.

Mathematical model

The antibody kinetics in vivo was described by a two-compartment non-recycling model in which blood and tumor are the two compartments. The flow between compartments was assumed to follow first-order kinetics and is defined by the transfer rate constants k_1, k_2 and k_3, representing the flow from blood to a generic body pool, from blood to the tumor, and from tumor to body pool, respectively. According to this model, the amount of radiolabeled antibody in the tumor is given by the function:

$$f(t) = \frac{U_{\max}(k_1 + k_2)}{k_3 - (k_1 + k_2)} \left(e^{-(k_1+k_2)t} - e^{-k_3 t} \right),$$

where $U_{\max}$ indicates the antibody uptake in the tumor. If data are expressed as % ID/g, then

$$U_{\max} = \frac{100}{M} \frac{k_2}{k_1 + k_2} [\%\mathrm{ID/g}],$$

where M is the tumor mass (g) and $k_2/(k_1 + k_2)$ is the ratio of injected activity flowing into the tumor.

The values of $U_{\max}$ and flow rate constants for the antibody were estimated using least-squares techniques by fitting the model function to the decay-corrected activity measurements in the tumors based on the regression algorithms of SigmaPlot software.

The cumulative activity of the ^{90}Y-labeled molecule per unit mass of the tumor was calculated as the integral of the time activity curve (AUC, area under the curve):

$$\mathrm{AUC} = \frac{100}{M} \frac{k_2}{k_3(k_1 + k_2)} [\%\mathrm{ID\,h/g}],$$

in which the model parameters were estimated from the tumor data without correction for radioactive decay.

Table 1 Description of in vivo experiments

Treatment	Experiment code				
	$1-^{111}$In	$1-^{90}$Y	$2-^{90}$Y	$3-^{90}$Y	$4-^{90}$Y
Non-tumor					
No. animals	ND	ND	ND	ND	21
No. animals per time point					3
A431 tMock					
No. animals	16	ND	18	24	21
Mean tumor weight ± SE (g)	0.574 ± 0.101		0.327 ± 0.072	0.296 ± 0.022	0.400 ± 0.078
No. animals per time point	4		3	4	3
A431 FR					
No. animals	16	15	18	24	35
Mean tumor weight ± SE (g)	0.386 ± 0.046	0.125 ± 0.044	0.362 ± 0.051	0.255 ± 0.036	0.510 ± 0.052
No. animals per time point	4	3	3	4	5
Injected dose					
Administered activity (kBq)	800	450	450	1,100	600
Specific activity (kBq/µg)	50	50	90	90	70
Interval times (h)	3/24/48/120	1/3/24/48/120	1/3/24/48/72/144	3/15/24/48/72/144	1/3/15/24/48/72/144
Organ assessed[a]	Blood, tumor, spleen, liver, kidneys, sternum, lungs, heart and muscles				

[a]In all but the $3-^{90}$Y experiment in which liver, chest and lung were not measured; the analysis of blood clearance was performed in A431FR- and A431tMock-bearing mice using data from ^{90}Y experiments 2, 3 and 4

Finally, the blood pharmacokinetics of ^{90}Y-mAb was described using the bi-exponential function: $y(t) = ae^{-\alpha t} + be^{-\beta t}$ to fit the non-corrected activity measurements in blood and was used to derive the blood terminal half-life ($t^{1/2}$ β).

The values in mice bearing A431FR or A431tMock were compared using a two-sided Student's *t*-test, pairing the experiments performed in parallel with the same radiolabeled preparation. Differences were considered significant at $P < 0.05$. Statistical analyses were performed using GraphPad software (GraphPad Software Inc, San Diego, CA, USA).

Results

All procedures and experiments were conducted under good laboratory practice (GLP) conditions on the premise of future clinical application of the ^{90}Y- and ^{111}In-mAb. In optimizing procedures to obtain functional radiolabeled mAb, the following parameters were considered: initial mAb concentration, L/P ratio, pH (5–7.5 range), incubation time (30–60 min), temperature (37–45°C), radioactive quantity (50–200 MBq/mg), use of ascorbic acid as a radioprotectant, and the effect of trace metal contaminants.

mAb derivatization with Bz-DOTA

Optimal initial mAb concentrations were essential to achieve efficient binding of the chelating agent Bz-DOTA to the reactive amino groups. We first used a mAb preparation at 10 mg/ml, but neither increased incubation time, temperature nor Bz-DOTA excess gave a substitution ratio sufficient for further labeling. The mAb concentration was brought to 75 mg/ml and in the range 40–75 mg/ml a linear increase in L/P ratio was achieved. However at the highest mAb concentration, binding activity following derivatization was compromised (data not shown). All subsequent studies were performed using a single preparation of certified mAb at 51 mg/ml. Bz-DOTA-MOv18 conjugates were prepared using different molar excesses which yielded different substitution ratios. The reaction buffer did not directly affect the L/P, but was important for the stability of the concentrated mAb during the reaction. SDS-PAGE confirmed an intact antibody with no aggregation. MALDI-TOF-MS was used for the quantitative assessment of Bz-DOTA/mAb ratios of these conjugates and demonstrated a high resolution in molecular mass determination. The MALDI-TOF-MS spectra were successfully recorded for each of the conjugates and mAb. Each spectrum contained one peak representing the mono-protonated molecule $(M+H)^+$. Due to the resolution of the MALDI-TOF-MS instrument, broad peaks were observed; the molecular mass of each conjugate or unmodified mAb was calculated from the peak centroid. Based on these results, L/P ratios as low as 0.5 and a proportional increase in the mass with increased L/P ratios were determined (Fig. 1). A 20-fold molar excess of Bz-DOTA gave a substitution ratio of up 7 (L/P mean 6.5), while a sixfold molar excess gave a mean L/P of 2.5 (range 1–4). The effect of L/P on functionality was assessed by immunofluorescence analysis on FR-positive IGROV1 cells. Overall, a Bz-DOTA substitution lower than four to five was well tolerated, since Bz-DOTA-mAb conjugates retained a binding activity essentially comparable to that of native mAb (Fig. 1). Binding assay on the FR-negative MeWo cells indicated the absence of non-specific binding (data not

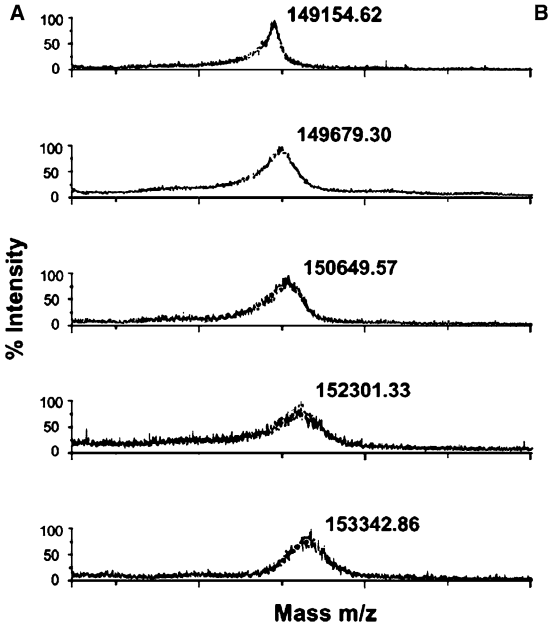

Fig. 1 **A** MALDI-TOF profile of representative derivatizations with Bz-DOTA and values of molecular mass of conjugates calculated from the peak centroid of the the mono-protonated molecule $(M+H)^+$. **B** Molar excess of Bz-DOTA and effect of L/P ratio on residual binding activity of Bz-DOTA-MOv18 conjugates as assessed by immunofluorescence analysis on live IGROV1 cells overexpressing the FR antigen. The functionality of the Bz-DOTA-mAb conjugates is given as % mean fluorescence intensity relative to that of the unmodified mAb

shown). Binding activity of Bz-DOTA-MOv18 stored at 4°C remained unchanged up to 6 months.

^{90}Y and ^{111}In radiolabeling and in vitro evaluation

Labeling yield was highest when Bz-DOTA-mAb concentrations were 7–10 mg/ml, with more diluted preparations resulting in very low incorporation yield (data not shown). Moreover, incorporation of ^{90}Y into Bz-DOTA-mAb conjugates was heavily affected by trace metal contaminants, so that treatment of all glassware and use of water with high resistivity for buffer preparations were required. At pH 7.5 and 37°C, the incorporation rate of ^{90}Y was considerably faster than in a more acid environment and at room temperature, and in these conditions, a high mean labeling yield as determined by ITLC before gel filtration (mean ± SE 85 ± 4%) was obtained in a short time. The use of a high ionic strength (0.5 M) prevented the formation of yttrium hydroxide colloids [23]. To further minimize radiolytic effects, ascorbic acid and HSA were added as radioprotectants during ^{90}Y labeling; accordingly, SDS-PAGE revealed intact mAb with no aggregates. When this procedure was omitted, integrity of the molecule was affected (data not shown). Minor modifications were necessary to achieve satisfactory labeling with ^{111}In, but even in optimized conditions, the labeling yield (mean ± SE 64 ± 3%) was lower than that for ^{90}Y. After desalting chromatography, radiolabeled mAb was at least 98% pure as indicated by ITLC; the remainder was present as a complex of EDTA or DTPA. When isotope:Bz-DOTA-mAb ratios of 100 and 50 MBq/mg were applied for ^{90}Y and ^{111}In, respectively, final mean specific activities of 74 and 37 MBq/mg were obtained. Analysis of immunoreactivity indicated that about 60% of ^{90}Y- or ^{111}In-MOv18 bound to cells overexpressing FR (mean ± SE in 16 experiments: 59.6 ± 3.9 and 58.1 ± 3.2% immunoreactivity for ^{90}Y-MOv18 and ^{111}In-MOv18, respectively). With all radiolabeled preparations, the curves presented a significant regression with P values < 0.001 and no binding over background was observed on FR-negative Mewo and A431tMock cells (data not shown), further indicating that binding specificity was maintained after labeling.

No bacterial contamination appeared after incubation of the peptone solution, indicating that the filtration unit and the filtrate solution of radiolabeled mAb were sterile. Pyrogen contamination based on the LAL assay was < 0.1 U/ml. Radiolabeled preparations incubated in human serum for 48 h lost 2.5 and 2.2% ^{90}Y and ^{111}In, respectively, and SDS-PAGE revealed no other labeled serum proteins, indicating absence of trans-chelation.

In vivo evaluation of radiolabeled MOv18 preparations

Three pairs of mice bearing A431FR or A431tMock tumors of comparable size in the left flank region were imaged with ^{111}In-MOv18. Figure 2 shows the scintigraphic images of a representative pair. Localization of ^{111}In-MOv18 in the A431FR tumor increased until 120 h (panel E), with evidence of early localization (panel B, thin arrow). By contrast, the blood pool localization (hypogastric region—thick arrow) decreased over time, and the A431tMock tumor was barely or not detectable at all time points examined. In parallel to scintigraphy, other tumor-bearing mice were sacrificed at the same time points (see Table 1). Data obtained from all dissected tumors are reported in Table 2 and used to generate Fig. 3, which represents the experimental accumulation of ^{111}In-Mov18 (% ID/g) in the xenografted tumors with time. In agreement with imaging results, maximal tumor uptake was higher in A431FR than in A431tMock tumors (U_{max} ± SE 45 ± 5 vs. 11.3 ± 1.6, respectively).

Figure 4 shows the biodistribution of ^{90}Y-MOv18 in tissue/organs of non-tumor and tumor-bearing mice from experiment 4–^{90}Y as % ID/g ± SE to illustrate the intra-assay variability; whereas the analytical data from the time interval common to all the experiments are given in Table 2 as % ID/g and tissue/organs:blood ratio to enable evaluation of inter-assay variability. The organ biodistribution in non-tumor bearing mice was comparable to that in A431tMock- and A431FR-bearing mice. In all experiments, MOv18 accumulation in sternum (bone), heart, lungs and kidney increased sharply until 3 h, slowly decreasing thereafter. In spleen, liver and muscle, the uptake was more stable over time. In the A431tMock-tumor tissue, maximum uptake was at 24–48 h (range 5–9% ID/g) followed by a very slow decrease. Despite inter-assay variability, localization in A431FR tumors was several-fold higher than in A431tMock tumors at all time intervals.

To evaluate the experimental accumulation of ^{90}Y-MOv18 (% ID/g) in the xenografted tumors over time, the mean tumor uptake was calculated according to the mathematical model described in Materials and Methods. As shown in Table 3, the values were about sevenfold higher in A431FR tumors (53.7 vs. 7.4% ID/g for A431FR and A431tMock, respectively) and significantly different ($P = 0.0332$). To enable comparison of effective total radiation to tumor mass, the raw data (not corrected for the physical decay) were used to calculate accumulated ^{90}Y activity in the tumor (AUC) for the A431FR and A431tMock groups; accumulation of ^{90}Y-MOv18 was sixfold higher ($P = 0.0465$) than in A431tMock (Table 3).

Blood terminal half-life ($t^{1/2}\beta$) in non-tumor mice (mean ± SE 51 ± 7 h) was similar to that calculated in the A431tMock-bearing mice (mean ± SE 66 ± 3 h), whereas the $t^{1/2}\beta$ in A431FR-bearing mice (mean ± SE 35 ± 3 h) was significantly shorter (A431FR vs. A431tMock: $P = 0.0339$). Consistent with the shorter $t^{1/2}\beta$, the % ID/g was lower in all tissue/organs except tumors of mice bearing A431FR tumors at the last time point examined (144 h). The blood $t^{1/2}\beta$ was in the range expected for whole murine radiolabeled

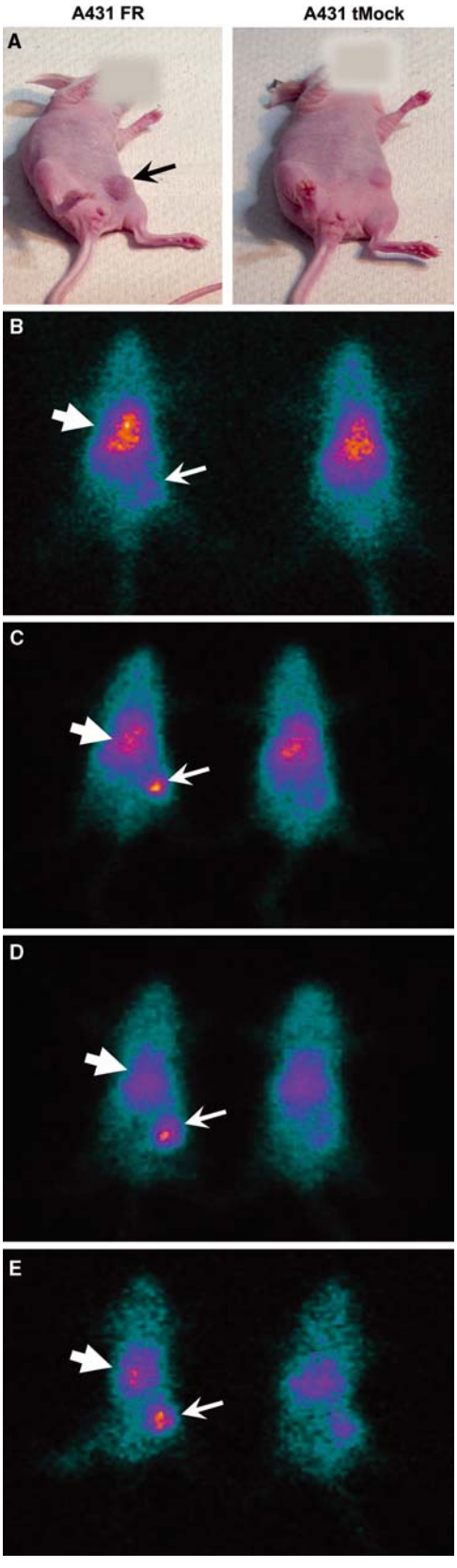

◀

Fig. 2 Localization of ^{111}In-MOv18 in two representative mice bearing A431FR (final weight 0.58 g) or A431tMock (final weight 0.50 g) subcutaneously in the left flank region. Light image at 3 h (**A**) and immunoscintigraphic images at 3 (**B**), 24 (**C**), 48 (**D**) and 120 (**E**) h after injection. The same animals were used for all images. *Thin arrow* A431FR tumors; *thick arrow* blood pool

mAbs, except in mice bearing FR-positive tumors, where $t^{1/2}\beta$ was shorter. This finding might rest in the sponge effect of tumors that highly overexpress FR, efficiently accreting the radiolabeled mAb and subtracting it from blood.

Discussion

For radioimmunotherapeutic applications, ^{90}Y must be linked as a metal complex to mAb via a suitable bifunctional chelating agent that has sufficient thermodynamic and kinetic stability to minimize release of the isotope and, in turn, in vivo toxicity. In the past, labeling chemistry with radiometals was limited until suitable chelating agents were developed, evolving from DTPA cyclic anhydride to backbone-substituted bifunctional DTPAs (Bz-DTPA, MX-DTPA and cyclohexyl-DTPA) and to bifunctional chelating agents based on the macrocyclic structure DOTA [31]. Derivatives of *p*-isothiocyanatobenzyl-1,4,7,10-tetraazacyclododecane-1,4,7,10- tetraacetic acid (Bz-DOTA) conjugated to mAbs have been shown to form highly stable complexes with yttrium and the lanthanide metal radionuclides for in vivo applications [7, 26, 34]. However, the routine use of Bz-DOTA-mAb conjugates has been frequently hampered by required lengthy synthesis of Bz-DOTA bifunctional chelates and by subsequent difficulties in ^{90}Y radiolabeling of these conjugates. Using MOv18 as entire murine mAb molecule, which could be concentrated up to 50 mg/ml without loss of functionality, we developed a simple procedure for both chelation and labeling that requires relatively short incubation time and mild conditions. This procedure preserved mAb functionality, as demonstrated in the in vivo preclinical model, and can be performed at the clinical site.

We used MALDI-TOF-MS, which allows accurate determination of average molecular mass and estimates molecular mass differences as low as 300 D, for the characterization of Bz-DOTA number on entire mAb conjugates [24]. The technique provided direct evidence of Bz-DOTA-mAb conjugation and, based on the molecular mass of Bz-DOTA and unmodified mAb, enabled estimates of L/P ratios or Bz-DOTA densities of the synthesized immunoreagent. This method represents a valid alternative to those currently in use to determine the average number of chelate per antibody molecule [12, 21, 27]. Complete functionality was preserved up to an L/P of 4–5; further increases in the L/P ratio resulted in a proportional loss of activity, probably due to interference of excessive numbers of chelator molecules with the antibody binding sites. The selected mean L/P substitution ratio, besides preserving tumor targeting properties, provided the best opportunity for ^{90}Y incorporation under optimized labeling conditions. The

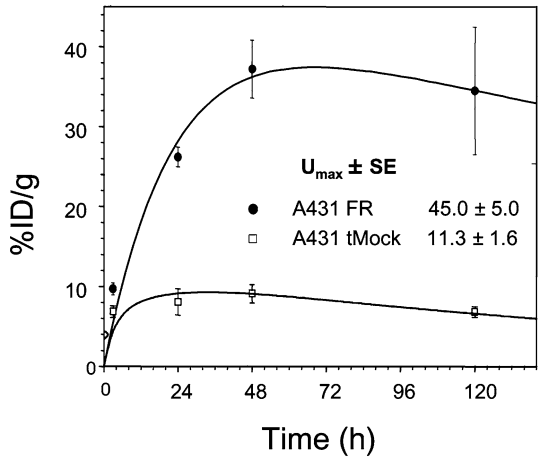

Fig. 3 Fitting curve used to calculate tumor uptake (U_{max}) of the mAb in A431FR- and A431tMock-bearing mice injected with ^{111}In-MOv18 (four animals for each time point)

chelation can be performed at the clinical site or, alternatively, might be carried out in bulk by a specialized center in light of the apparent long-term stability of the Bz-DOTA-mAb conjugates.

Efficient ^{90}Y incorporation also depended on avoiding trace metal contamination of glassware and buffers, in agreement with previous reports indicating that ^{90}Y incorporation into the free macrocyclic and acyclic chelators is most sensitive to the presence of trace levels of zinc and, to a lesser extent, ferrous and calcium ions [36]. However incorporation never exceeded 90%. This suggests the presence of minor amounts of unconjugated Bz-DOTA incompletely removed by initial gel filtration. Since our study was aimed at developing an in-house procedure for labeling under GLP conditions, we tried to avoid introducing procedures, such as dialysis, which are extremely difficult to perform under GLP conditions. Thus, we chose to perform a final gel filtration after radiolabeling to simultaneously enable removal of isotope,

Table 2 Biodistribution and tumor uptake of radiolabeled-MOV18, expressed as % ID/g and tissue/organ:blood ratio (T/B), following intravenous administration in athymic mice

Tissue/organ uptake at	Experiment code									
	1−^{111}In		1−^{90}Y		2−^{90}Y		3−^{90}Y		4−^{90}Y	
	% ID/g	T/B	% ID/g	T/B	% ID/g	T/B	% ID/g	T/B	% ID/g	T/B
Three (h)	Non tumor									
Blood	–	–	–	–	–	–	–	–	20.09	1
Tumor	–	–	–	–	–	–	–	–	–	–
Spleen	–	–	–	–	–	–	–	–	5.72	0.28
Kidneys	–	–	–	–	–	–	–	–	4.18	0.21
Liver	–	–	–	–	–	–	–	–	8.08	0.40
Sternum	–	–	–	–	–	–	–	–	2.33	0.12
Three (h)	A431 tMock									
Blood	29.28	1	–	–	26.68	1	26.46	1	12.76	1
Tumor	6.86	0.23	–	–	8.12	0.30	6.96	0.26	3.17	0.25
Spleen	4.97	0.17	–	–	6.02	0.22	5.49	0.21	5.49	0.43
Kidneys	6.39	0.22	–	–	6.26	0.23	5.91	0.22	4.79	0.38
Liver	7.85	0.27	–	–	10.11	0.38	7.98	0.30	10.24	0.80
Sternum	3.22	0.11	–	–	2.98	0.11	–	–	2.40	0.19
Three (h)	A431 FR									
Blood	30.12	1	23.33	1	25.37	1	27.54	1	22.63	1
Tumor	9.71	0.32	9.07	0.40	11.39	0.45	20.00	0.73	6.66	0.29
Spleen	5.42	0.18	4.42	0.19	3.92	0.15	6.00	0.22	6.83	0.30
Kidneys	8.35	0.28	6.27	0.27	4.68	0.18	5.65	0.21	5.21	0.23
Liver	9.35	0.31	10.35	0.44	8.98	0.35	7.48	0.27	10.25	0.45
Sternum	2.93	0.10	2.96	0.13	2.31	0.09	–	–	3.06	0.14
	% ID/g	T/B	% ID/g	T/B	% ID/g	T/B	% ID/g	T/B	% ID/g	T/B
24 (h)	Non tumor									
Blood	–	–	–	–	–	–	–	–	12.76	1
Tumor	–	–	–	–	–	–	–	–	–	–
Spleen	–	–	–	–	–	–	–	–	5.90	0.46
Kidneys	–	–	–	–	–	–	–	–	3.77	0.30
Liver	–	–	–	–	–	–	–	–	9.70	0.76
Sternum	–	–	–	–	–	–	–	–	2.10	0.16
24 (h)	A431 tMock									
Blood	13.26	1	–	–	8.92	1	16.97	1	12.47	1
Tumor	8.06	0.61	–	–	4.96	0.56	8.92	0.53	6.58	0.53
Spleen	5.20	0.39	–	–	3.92	0.44	6.18	0.36	5.43	0.44
Kidneys	7.82	0.59	–	–	3.45	0.39	4.71	0.28	3.90	0.31
Liver	7.91	0.60	–	–	9.67	1.08	6.17	0.36	9.59	0.77
Sternum	2.50	0.19	–	–	2.24	0.25	–	–	2.07	0.17
24 (h)	A431 FR									
Blood	13.65	1	16.47	1	7.49	1	13.24	1	11.76	1

Table 2 (Contd.)

Tissue/organ uptake at	Experiment code									
	1–^{111}In		1–^{90}Y		2–^{90}Y		3–^{90}Y		4–^{90}Y	
	% ID/g	T/B	% ID/g	T/B	% ID/g	T/B	% ID/g	T/B	% ID/g	T/B
Tumor	26.20	1.92	63.44	3.85	31.73	4.23	37.21	2.81	21.42	1.82
Spleen	6.16	0.45	7.09	0.43	4.57	0.61	5.21	0.39	6.82	0.58
Kidneys	6.16	0.45	4.62	0.28	2.70	0.36	3.58	0.27	3.99	0.34
Liver	11.15	0.82	10.86	0.66	9.34	1.25	5.94	0.45	9.65	0.82
Sternum	2.27	0.17	3.03	0.18	1.60	0.21	–	–	2.24	0.19
	% ID/g	T/B	% ID/g	T/B	% ID/g	T/B	% ID/g	T/B	% ID/g	T/B
48 (h)	Non tumor									
Blood	–	–	–	–	–	–	–	–	13.24	1
Tumor	–	–	–	–	–	–	–	–	–	–
Spleen	–	–	–	–	–	–	–	–	7.01	0.53
Kidneys	–	–	–	–	–	–	–	–	4.03	0.30
Liver	–	–	–	–	–	–	–	–	9.28	0.70
Sternum	–	–	–	–	–	–	–	–	2.08	0.16
48 (h)	A431 tMock									
Blood	11.10	1	–	–	9.94	1	13.47	1	8.57	1
Tumor	9.11	0.82	–	–	4.83	0.49	8.23	0.61	5.71	0.67
Spleen	5.69	0.51	–	–	10.62	1.07	6.22	0.46	5.75	0.67
Kidneys	7.01	0.63	–	–	3.22	0.32	3.49	0.26	2.81	0.33
Liver	8.96	0.81	–	–	9.13	0.92	5.74	0.43	12.02	1.40
Sternum	2.60	0.23	–	–	2.52	0.25	–	–	2.02	0.24
48 (h)	A431 FR									
Blood	10.91	1	15.92	1	3.45	1	9.54	1	8.58	1
Tumor	37.20	3.41	65.89	6.87	19.13	5.55	55.14	5.78	29.13	3.39
Spleen	6.53	0.60	7.90	0.55	4.40	1.27	7.83	0.77	6.92	0.81
Kidneys	5.97	0.55	3.86	0.24	2.23	0.65	3.29	0.34	3.04	0.35
Liver	12.25	1.12	9.07	0.91	12.75	3.70	5.95	0.62	9.84	1.15
Sternum	1.68	0.15	2.38	0.20	0.89	0.26	–	–	1.82	0.21
	% ID/g	T/B	% ID/g	T/B	% ID/g	T/B	% ID/g	T/B	% ID/g	T/B
120/144 (h)	Non tumor									
Blood	–	–	–	–	–	–	–	–	10.03	1
Tumor	–	–	–	–	–	–	–	–	–	–
Spleen	–	–	–	–	–	–	–	–	8.41	0.84
Kidneys	–	–	–	–	–	–	–	–	3.50	0.35
Liver	–	–	–	–	–	–	–	–	8.23	0.82
Sternum	–	–	–	–	–	–	–	–	1.97	020
120/144 (h)	A431 tMock									
Blood	8.68	1	–	–	4.82	1	10.40	1	10.54	1
Tumor	6.79	0.78	–	–	3.09	0.64	6.31	0.61	8.34	0.79
Spleen	4.27	0.49	–	–	5.73	1.19	6.82	0.66	7.27	0.69
Kidneys	5.09	0.59	–	–	2.40	0.50	2.48	024	3.00	0.28
Liver	7.41	0.85	–	–	6.78	1.41	4.46	0.43	8.18	0.78
Sternum	1.34	0.15	–	–	1.77	0.35	–	–	1.64	0.16
120/144 (h)	A431 FR									
Blood	5.90	1	6.39	1	0.49	1	3.04	1	4.16	1
Tumor	34.45	5.84	67.58	10.59	9.70	19.96	44.39	14.62	38.77	9.32
Spleen	6.30	1.07	4.45	0.70	2.98	6.13	4.14	1.36	4.97	1.19
Kidneys	4.27	0.72	2.39	0.38	0.81	1.66	1.41	0.46	1.66	0.40
Liver	7.43	1.26	5.42	0.87	3.74	7.70	2.63	0.86	5.05	1.21
Sternum	1.09	0.19	1.29	0.20	0.78	1.61	–	–	1.03	0.25

free or chelated by unbound Bz-DOTA, and addition of ascorbic acid and HSA as radioprotectants [6].

The experimental demonstration of optimal labeling conditions rests in the maintenance of binding activity as determined by comparative ELISA at the same molar concentrations of ^{90}Y-radiolabeled and unmodified antibodies. In these experimental conditions, the immunoreactivity was always $>80\%$ (data not shown). Parallel assay of the same radiolabeled preparation by ELISA and the more widely used Lindmo assay [25] revealed an apparent decrease in immunoreactivity to about 60% in the second assay. This apparent lower value is likely due to an underestimation of the immunoreactive fraction when the specific activity of the radiolabeled reagents is <74 MBq/mg. As a result, extrapolation of the cell-bound antibody fraction to infinite antigen excess could cause an underestimation of the immunoreactive fraction. Immunoreactivity was comparable on live cells expressing FR either naturally (IGROV1 ovarian carcinoma cells) or ectopically (A431FR cells). Furthermore, in contrast to a recent report [2], we observed no significant difference in

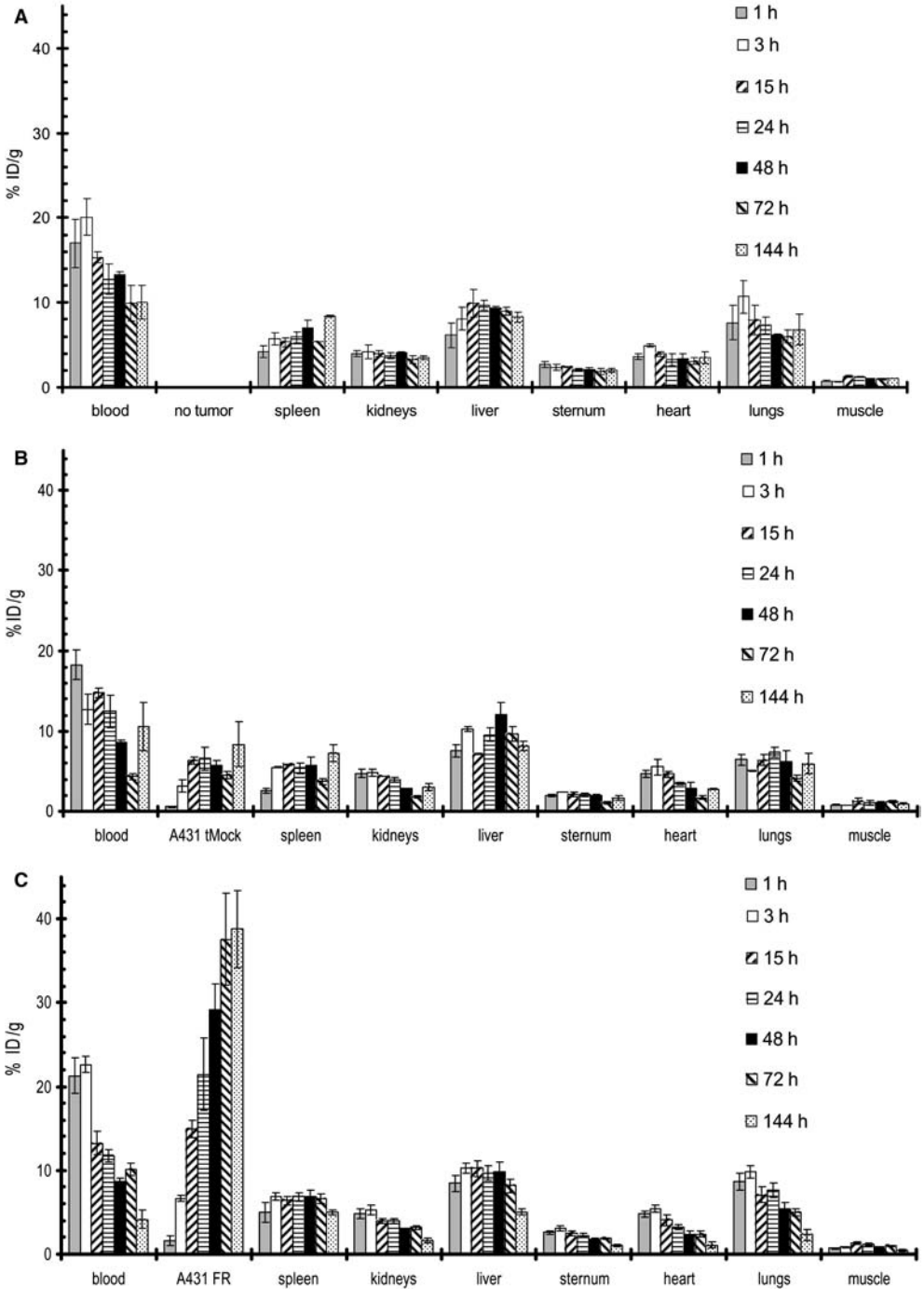

Fig. 4 Biodistribution of ^{90}Y-MOv18 in tissue/organs collected at different time points from non-tumor- (**A**), A431tMock- (**B**) and A431FR- (**C**) bearing mice. Values are expressed as mean % injected dose/g ±SE in groups of three to five animals for each time point

immunoreactivity when fixed instead of live cells were used. These data, together with biochemical analyses of numerous in vitro and in vivo samples from ovarian carcinoma (our unpublished data), suggest that the release of soluble FR in conditioned medium or in biological samples is negligible, if present at all, and not sufficient to interfere with MOv18 binding to its relevant target on the tumor cell surface.

The exceptional kinetic inertness of Bz-DOTA-type chelates has been documented [26, 36] and we calculated that less than 3% of ^{90}Y and ^{111}In were present as free metals after 48 h incubation of radiolabeled MOv18 with human serum. To indirectly evaluate the in vivo stability of radiolabeled MOv18, we examined the data obtained from the sternum since bone is a primary organ of accretion of lanthanide-like compounds such as yttrium [35]; in all of the in vivo experiments, the sternum:blood ratios were relatively constant for the time of observation (Table 2), indicating that the radioactivity in the bones derives from the plasma compartment and that the dissociation of ^{90}Y from mAb-chelate conjugates is negligible. Such stability is encouraging in the context of radioimmunotherapeutic applications.

Table 3 Tumor uptake and AUC values of ^{90}Y-MOv18 following intravenous administration in athymic mice bearing A431FR or A431tMock cells

Parameters	A431FR	A431tMock
Tumor U_{max} (% ID/g)		
Mean ± SE	53.7 ± 9.2	7.4 ± 1.2
t-test	$P = 0.0332$	
Tumor AUC (% ID/g/h)		
Mean ± SE	3,000 ± 600	540 ± 80
t-test	$P = 0.0465$	

The values, decay-corrected only for U_{max}, are from the three experiments in which pairing for the same radiolabeled preparation analysis was possible (see Table 1)

The described mild and short procedures for labeling with radiometals can be applied to other mAb, provided that they remain stable in solution at relatively high molar concentrations; accordingly, we have obtained promising results (high radiometal incorporation, > 50% immunoreactive fraction by Lindmo method and in vitro stability in human serum) with other anti-FR antibody-based reagents (unpublished observations).

The xenograft tumor model used for our in vivo preclinical evaluation enabled us to determine the specific antibody retention due to antigen recognition and, simultaneously, to exclude the non-specific uptake due to tumor growth characteristics. To this aim, we generated a pair of isogenic cell lines by transfecting A431 cells, known for a good take in athymic mice, with the target antigen (FR) or the empty vector. In the case of A431FR cells, we selected a subclone overexpressing FR at levels similar to those detected in in vivo human samples (twofold to fivefold higher than the mean expression value in cell lines). To better analyze the localization of ^{90}Y-MOv18 in the in vivo model and eventually to determine the dosimetry, tumor cells were grown as solid subcutaneous nodules. Uptake and adsorbed radiation dose in the tumor were assessed by a mathematical procedure that allows determination of tumor uptake (U_{max}) and AUC, parameters which are more appropriate than tumor/blood ratios or % ID/g at single time points to measure the localization and the effective total radiation dose to the tumor mass over time. Maximum uptake of ^{90}Y-MOv18 in A431FR tumors was sevenfold higher than in the FR-negative tumors ($P = 0.0332$); the tumor AUC of ^{90}Y-MOv18 was nearly sixfold higher ($P = 0.0465$). By contrast, the uptake by other tissues/organs was lower and decreased over time. Our FR-overexpressing preclinical model combined with the mathematical procedure used might serve as a basis of direct comparison with future MOv18 derivatives and anti-FR human reagents now being developed, independent of their blood clearance. Furthermore, use of the reported mathematical procedure might ultimately serve in estimating the therapeutic index of radiolabeled reagents and in designing more appropriate preclinical models, such as intraperitoneally growing ovarian carcinomas, to test their therapeutic efficacy.

Murine mAb are known to induce a human anti-mouse immunoglobulin antibody response, particularly evident in solid tumor patients and after multiple administrations [13, 29]. However, the remarkable response rate achievable with a single injection of radiolabeled mouse mAb suggests the promise of other murine mAbs that, like mAb MOv18, have a high targeting ability. Together these data indicate that the anti-ovarian carcinoma ^{90}Y- or ^{111}In-labeled MOv18, obtainable in GLP conditions at the clinic site, is directly amenable to clinical use. A phase I study to assess dosimetry and toxicity in advanced ovarian cancer patients is ongoing.

Further optimization of the three components of the radioimmunoconjugate is expected. For example, the β-emitting lanthanide ^{177}Lu ($T_{1/2} = 6.7$ days, $E_\gamma = 0.208$ MeV, $E_{\beta max} = 0.497$ MeV, max tissue penetration = 2.0 mm) might be considered for radioimmunotherapy due to its beta energy emission for cell killing, a physical half-life that better matches mAb pharmacokinetics, and the possibility of contemporaneous external imaging of tumor lesions (for dosimetry and treatment monitoring). The recent pharmaceutical availability of this radionuclide and the possibility of exploiting the same radiolabeling chemistry as with ^{90}Y should enable the preclinical evaluation of localization and therapeutic efficacy of ^{177}Lu-MOv18. Furthermore, we are developing completely human anti-FR antibody reagents to allow repeated treatment without inducing a human anti-mouse antibody response. Finally, the use of tissue-specific degradable peptide linkers [14] as a means to reducing radiation to normal tissues awaits further evaluation.

The present study with ^{90}Y-MOv18, together with previous encouraging clinical results with ^{131}I-MOv18, point to the promise of a radioimmunotherapeutic approach in the management of ovarian cancer. The selection of the isotope will be driven by the clinical setting, with the ^{90}Y-reagent, here described, finding potential use in consolidation therapy following suboptimal surgery (residual disease > 1 cm), and with ^{131}I-MOv18 or ^{177}Lu-MOv18 more suited in adjuvant therapy of minimal residual disease.

Acknowledgements The authors thank Gloria Bosco for manuscript preparation. This work was partially supported by AIRC-FIRC and a MIUR grant to Dompé.

References

1. Alvarez RD, Huh WK, Khazaeli MB, Meredith RF, Partridge EE, Kilgore LC, Grizzle WE, Shen S, Austin JM, Barnes MN, Carey D, Schlom J, LoBuglio AF (2002) A phase I study of combined modality (90)Yttrium-CC49 intraperitoneal radioimmunotherapy for ovarian cancer. Clin Cancer Res 8:2806–2811
2. Andersson H, Elgqvist J, Horvath G, Hultborn R, Jacobsson L, Jensen H, Karlsson B, Lindegren S, Palm S (2003) Astatine-211-labeled antibodies for treatment of disseminated ovarian cancer: an overview of results in an ovarian tumor model. Clin Cancer Res 9:3914S–3921S

3. Bischof Delaloye A (2003) The role of nuclear medicine in the treatment of non-Hodgkin's lymphoma (NHL). Leuk Lymphoma 44(Suppl 4):S29–S36
4. Bottero F, Tomassetti A, Canevari S, Miotti S, Ménard S, Colnaghi MI (1993) Gene transfection and expression of the ovarian carcinoma marker folate binding protein on NIH/3T3 cells increases cell growth in vitro and in vivo. Cancer Res 53:5791–5796
5. Casalini P, Luison E, Menard S, Colnaghi MI, Paganelli G, Canevari S (1997) Tumor pretargeting: role of avidin/streptavidin on monoclonal antibody internalization. J Nucl Med 38:1378–1381
6. Chakrabarti MC, Le N, Paik CH, De Graff WG, Carrasquillo JA (1996) Prevention of radiolysis of monoclonal antibody during labeling. J Nucl Med 37:1384–1388
7. Chappell LL, Ma D, Milenic DE, Garmestani K, Venditto V, Beitzel MP, Brechbiel MW (2003) Synthesis and evaluation of novel bifunctional chelating agents based on 1,4,7,10-tetraazacyclododecane-N,N′,N″,N‴-tetraacetic acid for radiolabeling proteins. Nucl Med Biol 30:581–595
8. Chinn P, Braslawsky G, White C, Hanna N (2003) Antibody therapy of non-Hodgkin's B-cell lymphoma. Cancer Immunol Immunother 52:257–280
9. Coney LR, Tomassetti A, Carayannopoulos L, Frasca V, Kamen BA, Colnaghi MI, Zurawski VR Jr (1991) Cloning of a tumor-associated antigen: MOv18 and MOv19 antibodies recognize a folate-binding protein. Cancer Res 51:6125–6132
10. Crippa F, Buraggi GL, Di Re E, Gasparini M, Seregni E, Canevari S, Gadina M, Presti M, Marini A, Seccamani E (1991) Radioimmunoscintigraphy of ovarian cancer with the MOv18 monoclonal antibody. Eur J Cancer 27:724–729
11. Crippa F, Bolis G, Seregni E, Gavoni N, Bombardieri E, Scarfone G, Ferrari C, Buraggi GL (1995) Single dose intraperitoneal radioimmunotherapy with the murine monoclonal antibody 131I-MOv18: clinical results in patients with minimal residual disease of ovarian cancer. Eur J Cancer 31A:686–690
12. Dadachova E, Chappell LL, Brechbiel MW (1999) Spectrophotometric method for determination of bifunctional macrocyclic ligands in macrocyclic ligand-protein conjugates. Nucl Med Biol 26:977–982
13. DeNardo GL, Bradt BM, Mirick GR, DeNardo SJ (2003) Human antiglobulin response to foreign antibodies: therapeutic benefit? Cancer Immunol Immunother 52:309–316
14. DeNardo GL, DeNardo SJ, Peterson JJ, Miers LA, Lam KS, Hartmann-Siantar C, Lamborn KR (2003) Preclinical evaluation of cathepsin-degradable peptide linkers for radioimmunoconjugates. Clin Cancer Res 9:3865S-3872S
15. Dixon KH, Mulligan T, Chung KN, Elwood PC, Cowan KH (1992) Effects of folate receptor expression following stable transfection into wild type and methotrexate transport-deficient ZR-75–1 human breast cancer cells. J Biol Chem 267:24140–24147
16. Epenetos AA, Hird V, Lambert H, Mason P, Coulter C (2000) Long term survival of patients with advanced ovarian cancer treated with intraperitoneal radioimmunotherapy. Int J Gynecol Cancer 10:44–46
17. Figini M, Ferri R, Mezzanzanica D, Bagnoli M, Luison E, Miotti S, Canevari S (2003) Reversion of transformed phenotype in ovarian cancer cells by intracellular expression of anti folate receptor antibodies. Gene Ther 10:1018–1025
18. Fogh J, Bean MA, Bruggen J (1978) Comparison of a human tumor cell line before and after growth in the nude mouse. In: Fogh J, Giovanella B (eds) The nude mouse in experimental and clinical research. Academic, New York, pp 215–234
19. Gadina M, Canevari S, Ripamonti M, Mariani M, Colnaghi MI (1991) Preclinical pharmacokinetics and localization studies of the radioiodinated anti-ovarian carcinoma MAb MOv18. Nucl Med Biol 18:403–408
20. Griffiths GL (1995) Cancer therapy with radiolabelled antibodies. In: Goldenberg DM (ed) Radiochemistry of therapeutic radionuclides. CRC Press, Boca Raton, Florida, p 47
21. Hnatowich DJ, Childs RL, Lanteigne D, Najafi A (1983) The preparation of DTPA-coupled antibodies radiolabeled with metallic radionuclides: an improved method. J Immunol Methods 65:147–157
22. Jemal A, Tiwari RC, Murray T, Ghafoor A, Samuels A, Ward E, Feuer EJ, Thun MJ (2004) Cancer statistics. CA Cancer J Clin 54:8–29
23. Kukis DL, DeNardo SJ, DeNardo GL, O'Donnell RT, Meares CF (1998) Optimized conditions for chelation of yttrium-90-DOTA immunoconjugates. J Nucl Med 39:2105–2110
24. Lewis MR, Raubitschek A, Shively JE (1994) A facile, water-soluble method for modification of proteins with DOTA. Use of elevated temperature and optimized pH to achieve high specific activity and high chelate stability in radiolabeled immunoconjugates. Bioconjug Chem 5:565–576
25. Lindmo T, Boven E, Cuttitta F, Fedorko J, Bunn PA Jr (1984) Determination of the immunoreactive fraction of radiolabeled monoclonal antibodies by linear extrapolation to binding at infinite antigen excess. J Immunol Methods 72:77–89
26. McMurry TJ, Brechbiel M, Kumar K, Gansow OA (1992) Convenient synthesis of bifunctional tetraaza macrocycles. Bioconjug Chem 3:108–117
27. Meares CF, McCall MJ, Reardan DT, Goodwin DA, Diamanti CI, McTigue M (1984) Conjugation of antibodies with bifunctional chelating agents: isothiocyanate and bromoacetamide reagents, methods of analysis, and subsequent addition of metal ions. Anal Biochem 142:68–78
28. Miotti S, Canevari S, Ménard S, Mezzanzanica D, Porro G, Pupa SM, Regazzoni M, Tagliabue E, Colnaghi MI (1987) Characterization of human ovarian carcinoma-associated antigens defined by novel monoclonal antibodies with tumor-restricted specificity. Int J Cancer 39:297–303
29. Miotti S, Negri DRM, Valota O, Calabrese M, Bolhuis RLH, Gratama JW, Colnaghi MI, Canevari S (1999) Level of anti-mouse antibody response induced by bispecific monoclonal antibody OC/TR in ovarian carcinoma patients is associated with longer survival. Int J Cancer 84:62–68
30. Miotti S, Bagnoli M, Tomassetti A, Colnaghi MI, Canevari S (2000) Interaction of folate receptor with signaling molecules lyn and $G\alpha_{13}$ in detergent-resistant complexes from the ovary carcinoma cell line IGROV1. J Cell Sci 113:349–357
31. Moi MK, DeNardo SJ, Meares CF (1990) Stable bifunctional chelates of metals used in radiotherapy. Cancer Res 50:789s–793s
32. Ozols RF, Bookman MA, Connolly DC, Daly MB, Godwin AK, Schilder RJ, Xu X, Hamilton TC (2004) Focus on epithelial ovarian cancer. Cancer Cell 5:19–24
33. Paganelli G, Belloni C, Magnani P, Zito F, Pasini A, Sassi I, Meroni M, Mariani M, Vignali M, Siccardi AG, Fazio F (1992) Two-step tumor targetting in ovarian cancer patients using biotinylated monoclonal antibodies and radioactive streptavidin. Eur J Nucl Med 19:322–329
34. Peterson JJ, Pak RH, Meares CF (1999) Total solid-phase synthesis of 1,4,7,10-tetraazacyclododecane-N,N′,N″,N‴-tetraaceticacid- functionalized peptides for radioimmuno-therapy. Bioconjug Chem 10:316–320
35. Srivastava SC (1996) Criteria for the selection of radionuclides for targeting nuclear antigens for cancer radioimmunotherapy. Cancer Biother Radiopharm 11:43–50
36. Stimmel JB, Stockstill ME, Kull FC Jr (1995) Yttrium-90 chelation properties of tetraazatetraacetic acid macrocycles, diethylenetriaminepentaacetic acid analogues, and a novel terpyridine acyclic chelator. Bioconjug Chem 6:219–225
37. Toffoli G, Cernigoi C, Russo A, Gallo A, Bagnoli M, Boiocchi M (1997) Overexpression of folate binding protein in ovarian cancers. Int J Cancer 74:193–198

38. United Kingdom Co-ordinating Committee on Cancer Research (UKCCCR) (1998) Guidelines for the welfare of animals in experimental neoplasia, 2nd edn. Br J Cancer 77:1–10
39. van Zanten-Przybysz I, Molthoff CF, Roos JC, Plaizier MA, Visser GW, Pijpers R, Kenemans P, Verheijen RH (2000) Radioimmunotherapy with intravenously administered 131I-labeled chimeric monoclonal antibody MOv18 in patients with ovarian cancer. J Nucl Med 41:1168–1176
40. van Zanten-Przybysz I, Molthoff CF, Roos JC, Verheijen RH, van Hof A, Buist MR, Prinssen HM, den Hollander W, Kenemans P (2001) Influence of the route of administration on targeting of ovarian cancer with the chimeric monoclonal antibody MOv18: i.v. vs. i.p. Int J Cancer 92:106–114